ELECTRON-BEAM DIAGNOSTICS DEVELOPMENT FOR THE LOS ALAMOS FEL FACILITY*

M. D. Wilke, A. H. Lumpkin,** P. G. O'Shea, E. J. Pitcher and R. B. Feldman
Los Alamos National Laboratory
Los Alamos, New Mexico 87545 USA

Argonne National Laboratory, Advanced Photon Source**
Argonne, Illinois 60439 USA

Abstract

We describe some electron-beam diagnostics and results from the Los Alamos APLE Prototype Experiment (APEX) linac. The diagnostics include complementary nonintercepting and intercepting techniques with time integrated and time resolved capabilities.

Introduction

APEX is a photoinjector-RF linac, free electron laser (FEL) experimental facility that has been constructed as a prototype facility for techniques and diagnostics to be used on the Strategic Defense Initiatives Average Power Experiment (APLE) demonstration experiment presently being designed by Boeing. APEX is described in detail elsewhere [1,2].

The standard diagnostics include Optical Transition Radiation (OTR) screens, wall current monitors and magnetic spectrometers. All but the first wall current monitor will soon be converted to beam position monitors [3]. The screens are viewed by various vidicon, SIT, intensified CID and streak cameras. Several other techniques are used to measure the beam properties.

Figure 1 schematically shows some of the techniques in the vicinity of screen 4 just before the 60 degree bend between the accelerator and resonator sections, which we will describe in more detail.

OTR Screens and Emittance Measurements

OTR screens are used to measure beam position and size. We have tried several types of materials for the screens including 100 μm to 200 μm polished Mo, Si, Al and Al coated quartz. We also use 0.8 μm Al as the first foils of OTR interferometers. In all cases we find that damage nominally begins for macropulses greater than 10 μs and charge greater than 5 nC per micropulse when focused to about 300 μm diam. spots.

APEX is a low emittance accelerator and is capable of focusing beam waists of less than 100 μm. Resolution of these images is difficult and approaches the physical limitation of the OTR technique. Assuming the majority of

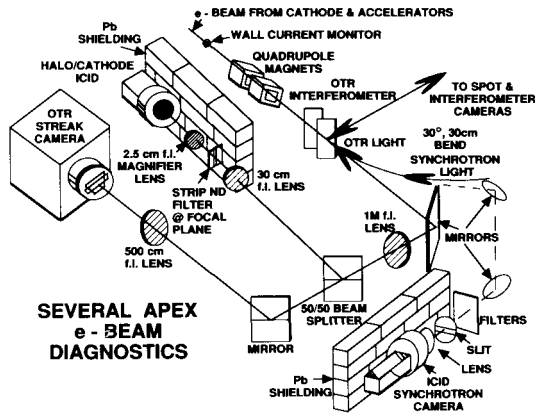

Fig. 1 Schematic of the diagnostics near the beginning of the 60 degree bend.

OTR light is emitted in a cone three times the angle of peak emission, with an equivalent f-number of $f = \gamma/6 = 13$, the resolution is diffraction limited in the visible ($\lambda = 600$ nm) to

$$\delta x = 2.44 \bullet f \bullet \lambda = 18\ \mu m.$$

On-line emittance measurements are important to determine machine performance versus parameter settings and for comparison of beam quality with the FEL performance for modeling purposes. We have recently begun measuring emittance by varying quadrupole currents and measuring the resulting spot size versus current at a downstream OTR screen. The measured spot sizes are then fit with a calculated curve to determine the emittance [4]. We have coupled the scanning process to EPICS automated control of APEX [5]. An example is shown in Figure 2. Also shown in Figure 2 are two curves with slightly different RMS emittance values in units of π-mm-mrad to indicate the sensitivity of the technique. The error bar is the RMS deviation of the best fit to the data.

The automated scan technique typically averages profiles from several macropulses at each quad setting to improve signal to noise. In the past, we have used an OTR interferometer to measure the beam divergence along with the minimum spot size and hence the emittance [6]. The OTR interferometer has the potential to yield an emittance figure on each macropulse and thereby determine emittance jitter. We are currently attempting to automate this technique.

*Work supported by the U.S. Army Strategic Defense Command under the auspices of the U.S. Department of Energy at Los Alamos National Laboratory.

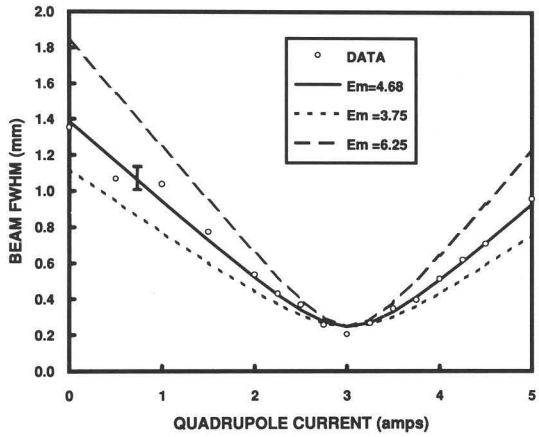

Fig. 2 Plots of fits to quadrupole scan data for determining emittance.

Streak Camera Micropulse Measurements

The combination of the OTR light and the RF-synchronously scanned streak camera provides a powerful tool for measuring the micropulse properties averaged over a macropulse [7]. Figure 1 shows the optical setup for imaging the back side of screen 4 onto the slit of the streak camera. The camera is deflected synchronously with the 108 MHz RF.

In Figure 3, we have plotted the pulse length versus micropulse charge for two photocathode laser spot diameters and 20 usec macropulses. The e-beam energy was 39 MeV and the drive laser had an 8 psec pulse width. We have deconvolved the 3.5 psec time resolution of the streak camera. Note the very narrow e-beam pulses lengths at low charges that result from the RF bunching when the electron pulses are phased on the rising amplitude of the RF.

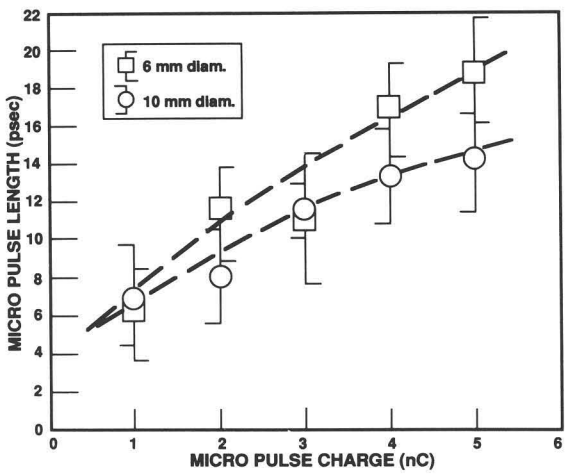

Fig. 3 Plot of the micropulse length versus micropulse charge.

Using the streak camera, we believe we have directly observed the effects of transverse wake fields on the micropulses. Transverse wake field effects have been predicted on APEX [8]. They can be generated by steering the e-beam off center through the accelerator. They also occur because of asymmetries in the accelerator or beam tube. The transverse wakes cause the tail of the electron bunch to be steered transversely. The effect increases with micropulse charge and the transverse size of the bunch. Figure 4 shows the effect on the streak image of steering a beam several millimeters off center through the last two accelerators. The beam is steered back to the center of screen 4 where the last set of quads was used to focus to a nominally 1.5 mm wide by 5 mm high spot. The 41 MeV beam was about 3 mm wide by 2 mm high through the accelerators with 4 nC/micropulse. The photocathode drive laser had an 11 psec pulse width.

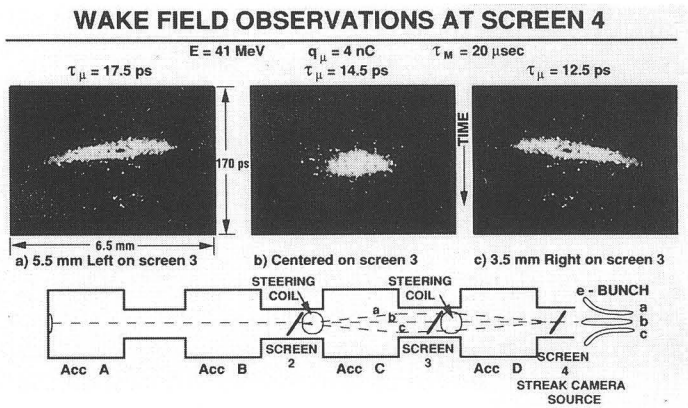

Fig. 4 Streak images showing micropulse effects of transverse wake fields.

The orientation of the images in Figure 4 is such that the x-axis is equivalent to looking at screen 4 in the direction away from the accelerators. It can be seen in Figure 4 that the image at screen 4 broadens when the beam is steered off center and also that the tail of the beam is kicked toward the near side of the accelerator. There was no measureable change in the micropulse length. A small amount of skew can be seen in the centered image as well. The skew on center is believed to be caused by asymmetric distribution of the APEX RF coupling cavities in the accelerators. Data taken at 5 nC with larger beam diameters through the accelerators shows a large amount of skew in the image when the beam is centered through the accelerators. Calculations estimating the wake field effects are underway and have so far reproduced the qualitative features of the measurements [9].

The larger spot sizes when the e-beam is focused on a screen translate into increased emittance due to the wakes. We also demonstrated that by steering slightly to the right on screen 4, we could compensate for accelerator asymmetries and produce a narrower spot.

Other Measurements

Beam halo is important in the construction of high-duty-factor machines, such as APLE, where halo interaction with the beam tube and accelerator could cause a significant radiation background and potentially activate the machine for long

periods of time. Figure 1 shows the optical setup for measuring halo used at APEX. The beam is focused at screen 4 and the OTR light is imaged onto a neutral density (ND) filter strip. The strip image is then magnified and reimaged on the ICID. The image region to the sides of the ND strip is not attenuated so that the lower intensity halo becomes visible.

Figure 5 shows normalized plots of line averages from halo images for several macropulse lengths where the center

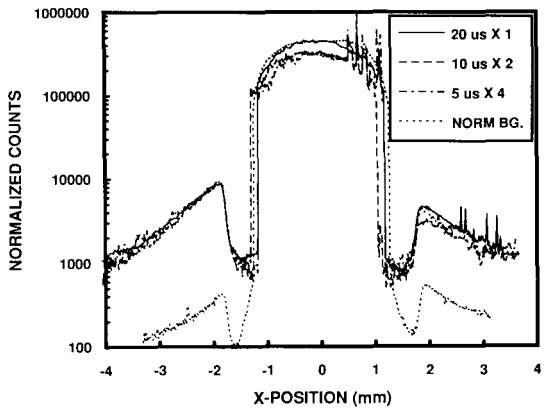

Fig. 5. Plots of processed halo data.

of the plot was multiplied by 100 to account for the ND 2.0 filter. The halo fraction is a constant indicating that the halo probably does not result during macropulse rise and fall. Modeling has reproduced the features the halo images but long computer runs are required because of the low statistics.

Synchrotron radiation from the beam provides a means for non-interceptive monitoring of the beam quality and position at bends in the transport. We have experimented with this technique at the first 30 degree section of the 60 degree bend as shown in Figure 1. It is possible to determine the shape of the beam and relative position, but determining the absolute position is difficult because of lack of references. We have also investigated the sensitivity of our technique by lowering the accelerator energy. The signal falls rapidly because of the γ^4 dependence of the total synchrotron power and the $1/\gamma^3$ dependence of the critical wavelength of emission. For ICID cameras the minimum beam energy for imaging is about 23 MeV.

OTR imaging has proven useful for determining field emission from the photocathode injector. Because the emittance of APEX is so low, the electron emission distribution of the cathode is reproduced on the second screen. We have compared images of a few micropulses of known charge with those when just the RF was operating. From the comparison we have determined a value of 0.045 nC per micropulse of RF which appeared mainly from a scratch in the photocathode substrate that was clearly reproduced on the OTR image.

Acknowledgments

The authors thank Scott Apgar and Clint Webb for their technical support and we thank Bruce Carlsten, Mark Schmitt and John Goldstein for calculational support. The authors also thank the other members of the APEX team for their cooperation and support including Don Feldman, Jim Early, Steve Bender, Nathan Okamoto, Mike Feind, Pat Schaffstall, Tom Zaugg, Paul Ortega and Laurel Conner. Special thanks to Kathy Derouin and Gerald Martinez for assistance in preparation of the document.

References

[1] Feldman, D. W., Bender, S. C., Carlsten, B. E., Early, J., Feldman, R. B., Goldstein, J. C., O'Shea, P. G., Pitcher, E., Schmitt, M. J., Stein, W. E., Wilke, M., and Zaugg, T., "Operation of the APEX Photoinjector Accelerator at 40 MeV", in these proceedings.

[2] O'Shea, P. G., Bender, S. C., Byrd, D. A., Carlsten, B. E., Early, J. W., Feldman, D. W., Feldman, R. B., Johnson, W. J. D., Lumpkin, A. H., Schmitt, M. J., Springer, R. W., Stein, W. E. and Zaugg, T. J., "Initial Results from the Los Alamos Photoinjector-Driven Free-Electron Laser", Nucl. Instr. and Meth., p52, A318, (1992).

[3] Gilpatrick, J. D., Martinez, R., Meyer, R. E., Power, J. F., Shurter, R. B., Wells, F. D., Johnson, K. F., Lloyd, S. and Neuschaefer, G. H., "Measurements and Performance of a Microstrip Beam Probe System," LA-UR-1428, (1991).

[4] Ross, M. C., Phinney, N., Quickfall, G., Shoaee, H. and Sheppard, J. C., "Automated Emittance Measurements in the SLC", Proc. 1987 IEEE Part. Accel. Conf., p725 V2, (1987).

[5] Pitcher, E., "Quad Scan Analysis Routine: ESAPII", Los Alamos Memorandum APEX:92-069, June 4, 1992.

[6] Rule, D. W., Fiorito, R. B., Lumpkin, A. H., Feldman, R. B. and Carlsten, B. E., "Comparative Analysis of Optical-Transition-Radiation-Based Electron-Beam Emittance Measurements for the Los Alamos Free-Electron Laser," Nucl. Inst. and Meth., A296 p. 739(1990).

[7] Lumpkin, A. H., "The Next Generation of RF FEL (Free Electron Laser) Diagnostics: Synchroscan and Dual-Sweep Streak Camera Techniques", Nucl. Instr. and Meth., A304 p. 31 (1991).

[8] Carlsten, B. E., Goldstein, J. C., Pitcher, E. J., Schmitt, M. J., "Simulations of APEX Accelerator Performance in the New Nonthermalized Photoinjector Regime. submitted to Nucl. Inst. Meth. A.

[9] Carlsten, B. E., private communication.